A comparative study on the mechanical properties, autogenous shrinkage and cracking proneness of alkali-activated concrete and ordinary Portland cement concrete

Li, Zhenming; Delsaute, Brice; Lu, Tianshi; Kostiuchenko, Albina; Staquet, Stéphanie; Ye, Guang

DOI
10.1016/j.conbuildmat.2021.123418

Publication date
2021

Document Version
Final published version

Published in
Construction and Building Materials

Citation (APA)
Li, Z., Delsaute, B., Lu, T., Kostiuchenko, A., Staquet, S., & Ye, G. (2021). A comparative study on the mechanical properties, autogenous shrinkage and cracking proneness of alkali-activated concrete and ordinary Portland cement concrete. *Construction and Building Materials*, *292*, 1-11. Article 123418. https://doi.org/10.1016/j.conbuildmat.2021.123418

Construction and Building Materials 292 (2021) 123418

Contents lists available at ScienceDirect

Construction and Building Materials

journal homepage: www.elsevier.com/locate/conbuildmat

A comparative study on the mechanical properties, autogenous shrinkage and cracking proneness of alkali-activated concrete and ordinary Portland cement concrete

Zhenming Li [a,*], Brice Delsaute [b], Tianshi Lu [d], Albina Kostiuchenko [a], Stéphanie Staquet [b], Guang Ye [a,c]

[a] Department of Materials and Environment (Microlab), Faculty of Civil Engineering and Geoscience, Delft University of Technology, Delft, The Netherlands
[b] BATir Department, Université Libre de Bruxelles, Brussel, Belgium
[c] Magnel Laboratory for Concrete Research, Department of Structural Engineering, Ghent University, Ghent, Belgium
[d] School of Civil Engineering and Geomatics, Southwest Petroleum University, Chengdu, China

HIGHLIGHTS

- Alkali-activated concrete (AC) reacts faster than OPC concrete (OC) in the very early age. In later age, however, OC shows higher degree of reaction.
- AC has lower tensile strength-to-compressive strength ratios than OC.
- AC shows higher autogenous shrinkage but later cracking time than OC. Nonetheless, the reaction degrees of the two systems at cracking are quite similar.
- AC shows much larger creep coefficient than OC.

ARTICLE INFO

Article history:
Received 26 September 2020
Received in revised form 5 April 2021
Accepted 7 April 2021

Keywords:
Mechanical properties
Autogenous shrinkage
Modelling
Creep
Alkali-activated concrete
OPC concrete

ABSTRACT

This study aims to compare the developments of mechanical properties and autogenous shrinkage related properties of alkali-activated materials-based concrete (AC) and ordinary Portland cement-based concrete (OC) against curing age and degree of reaction. Temperature Stress Testing Machines are utilized to monitor the evolution of the internal tensile stress and the cracking occurrence in the restrained concrete. It is found that AC shows lower tensile strength-to-compressive strength ratios than OC. The mechanical properties of both OC and AC can be modelled by a power law against the degree of reaction. AC shows higher autogenous shrinkage, but later cracking than OC when under restrained condition. However, the degrees of reaction at which AC and OC cracked are very similar. From the autogenous shrinkage, the elastic modulus and the self-induced stress, the elastic and creep deformations of the concrete can be calculated. AC is found to show much higher creep coefficient than OC.

1. Introduction

Ordinary Portland cement (OPC) based concrete has been the most widely used material in the world for a century [1]. The structures made from concrete are proven safe and durable. In recent years, however, the concern about global warming and carbon emission has been growing. An important part of global CO_2 emission comes from the construction sector, especially the production of cement. It has been reported that the cement production contributes to 5–8% CO_2 emission worldwide [2,3]. Up to now, lots of efforts have been made by academic and industrial communities to develop alternative binder materials to ordinary Portland cement [4,5]. Amongst all the alternatives, alkali-activated materials (AAMs), especially those made of industrial by-products such as granulated blast furnace slag and coal fly ash, are attracting increasing attention.

NaOH and Na_2SiO_3 activated concrete based on slag and fly ash can show high strength and good chemical resistance [6–8]. However, the autogenous shrinkage of these systems is normally high even at high water/binder ratios (e.g., 0.4–0.5). For example, Cartwright et al. [9] reported that the autogenous shrinkage of alkali-activated slag (AAS) mortar can be 5 times higher than that of OPC mortar. Partially replacing slag by fly ash normally results in a lower autogenous shrinkage [10–13]. However, compare to that of OPC systems with similar water/binder ratios or similar strength, the autogenous shrinkage of alkali-activated slag-fly ash

* Corresponding author.

https://doi.org/10.1016/j.conbuildmat.2021.123418
0950-0618/

(AASF) system is still much higher [14]. The high autogenous shrinkage has been considered as a main drawback of AAS and AASF materials, since it has a potential to induce micro- or macro- cracking of the concrete when used under restrained conditions [15].

In practise, concrete is always under a certain restraint provided by the rebar or adjacent components. However, it should be noted that the cracking proneness of concrete under restrained condition is actually determined by multiple factors, including shrinkage (due to thermal, autogenous or drying effect), creep, elastic modulus and tensile strength [16]. It is unable to claim that alkali-activated materials-based concrete (AC) would have high cracking proneness simply based on the free shrinkage results. The developments of mechanical properties of AC have to be considered in order to evaluate the cracking proneness. For a better understanding of the performance of AC, ordinary Portland cement-based concrete (OC) system whose behaviours have been known had better be used as reference. Therefore, comparative studies on the mechanical properties and cracking tendencies of AC and OC would be helpful for researchers to understand and benchmark AC. However, up to now, no published study can be found dealing with these issues.

With this background, this study is conducted to provide a direct comparison between the mechanical property's developments and autogenous shrinkage-induced cracking tendencies of AC and OC. In this study, two types of AC (AAS and AASF concrete) and three types of OC (CEM I, CEM III/A and CEM III/B concrete) with comparable 28-days compressive strength are prepared. Tensile strength and elastic modulus of the systems are studied. Temperature Stress Testing Machines (TSTMs) are used to measure the internal tensile stress and the cracking time of both series of concrete under restrained conditions. The creep coefficients of the concrete mixtures are then calculated from the experimental results and are compared.

2. Materials and methods

2.1. Raw materials and mixtures

2.1.1. Raw materials

AC was produced in Technische Universiteit Delft (TUD) while OC was produced in Université Libre de Bruxelles (ULB).

The precursors used for AC were slag and Class F fly ash [17]. The raw materials were supplied by Ecocem Benelux BV and Vliegasunie BV, respectively. X-ray fluorescence (XRF) was used to characterize the chemical compositions of the raw materials, as shown in Table 1. The density of slag and fly ash was 2.89 g/cm^3 and 2.44 g/cm^3, respectively. Alkaline activator was a combination of NaOH pellets, deionized water and Na_2SiO_3 solution. Every 100 g of activator contained 13.8 g of SiO_2 and 9.4 g of Na_2O and 76.8 g of water (i.e., M_S = 1.5).

Three types of cement were used to make OC: CEM I 52.5 N, CEM III/A 42.5 LA and CEM III/B 42.5 HSR LA. The slag/binder ratios in these three types of cement were 0%, 42.5% and 71%, respectively. The chemical compositions of the cements determined by XRF are also shown in Table 1 [18]. The slag used in CEM III/A and CEM III/B had nearly the same composition as the slag used in AC. The density of the three types of cement is 3.09 g/cm^3, 3.01 g/cm^3 and 2.93 g/cm^3, respectively. The contents of clinker, slag and limestone filler in each cement are shown in Table 2 [18].

2.1.2. Mixtures proportions

The mixture proportions of AC and OC are shown in Table 3 and Table 4, respectively. The aggregate contents of each size range in the two series of concrete prepared in the two laboratories are not exactly the same. However, the aggregate grades and the total volume fractions of the aggregate in AC and OC are similar, as shown in Tables 3 and 4. Therefore, the slight difference in the aggregate contents are believed to have limited influence on the reaction kinetics and properties of these two series of concrete. The final setting times of the mixtures are also shown in the tables.

2.2. Experimental methods

2.2.1. Degree of reaction

The reaction degree of the concrete mixtures at a certain time t was defined as the ratio between the corresponding reaction heat to the ultimate reaction heat. The ultimate heat at an infinite time was determined by extrapolation of the experimentally measured reaction heat. The detailed procedure to measure the reaction heat of AC and OC can be found in [19,20], respectively.

2.2.2. Strength

The compressive and splitting tensile strengths of AC were measured on concrete cubes with diameters of 150 × 150 × 150 mm^3 according to NEN-EN 12390 [21]. The measuring ages were 1, 3, 7, 28 days and the date when cracking of the beam in TSTM occurred. Compressive tests of OC were performed on cylindrical samples with a diameter of 98 mm and a height of 200 mm according to NBN-B 15-220 [22]. The splitting tensile strength was determined on cylinders with a diameter of 98 mm and a height of 150 mm according to NBN-B 15–218 [23]. The measurements were conducted at the age of 1, 3, 7 and 28 days. Three samples were tested for compressive and splitting strength at each curing age. According to [24] and [25], the compressive and splitting tensile strength of concrete cylinder is generally equal to 0.8 times of the strength of concrete cubes. Therefore, the strength results of AC obtained on cubes were multiplied by 0.8 to be compared with the strength results of OC which was obtained on cylinders.

2.2.3. Elastic modulus

A hydraulic Instron was used to measure the elastic modulus of AC in prisms (100 × 100 × 400 mm^3) as shown Fig. 1 (a). The measurement was conducted at the same ages as the strength tests. Three specimens were tested for each mixture at each age. The elastic modulus of OC were performed on samples with a diameter of 98 mm and a height of 350 mm according to NBN B 15–203 [26], as shown in Fig. 1 (b). Three specimens were tested for each mixture at each age. Unlike the compressive and splitting tensile strength, the elastic modulus results obtained in the two labs can

Table 1
Chemical compositions of slags, fly ash and clinker.

Precursor	Component (mass% as oxide)								
	SiO_2	Al_2O_3	CaO	MgO	Fe_2O_3	SO_3	K_2O	TiO_2	Other
Slag (TUD)	31	13	41	9	0.5	1	0.3	1	2
Fly ash (TUD)	57	24	5	2	7	0.3	2	1	3
Cement (ULB)	19	5	66	0.8	4	2	1	0.4	2
Slag (ULB)	34	12	40	9	0.3	3	0.4	0.6	2

Table 2
Cements characteristics.

	CEM I	CEM III/A	CEM III/B
Clinker content (%)	95*	58	27
Slag content (%)	–	42	71
Limestone filler content (%)	–	–	2

*The CEM I cement contained 5% of gypsum.

Table 3
Mixture proportions of AC (kg/m^3).

Mixtures	AAS	AASF
Slag	400	200
Fly ash	0	200
Activator	200	200
Aggregate [0–4 mm]	789	789
Aggregate [4–8 mm]	440	440
Aggregate [8–16 mm]	525	525
Volume fraction of aggregate	0.67	0.67
Final setting time	35 min	103 min
Density (kg/m^3)	2180	2150

Table 4
Mixture proportions of OC (kg/m^3).

Mixtures	CEM I	CEM III/A	CEM III/B
Cement	375	375	375
Water	165	167	165
Total water	169	169	169
Aggregate [0–3 mm]	722	722	722
Aggregate [2–6 mm]	311	311	311
Aggregate [6–10 mm]	438	438	438
Aggregate [10–14 mm]	415	415	415
Volume fraction of aggregate	0.71	0.71	0.71
Superplasticizer (Sika viscocrete 4, sulfonated naphthalene condensate)	5.63	2.63	5.25
Final setting time	9.0 h	8.8 h	10.5 h
Air content (%)	2.1	1.7	2.0
Density (kg/m^3)	2410	2410	2400

be directly compared due to the little effect of the specimen shape on the measured elastic modulus as demonstrated in [27,28].

2.2.4. Autogenous shrinkage

The measurement of autogenous shrinkage of AC was conducted in TUD by an Autogenous Deformation Testing Machine (ADTM). The details of the ADTM were given in [29]. The autogenous shrinkage of OC was measured in ULB, with the details of the testing device given in [30].

2.2.5. Autogenous shrinkage-induced stress

The development of tensile stress and cracking initiation of AC and OC induced by restrained autogenous shrinkage were tested by TSTMs in TUD and ULB, respectively. The details of the TSTMs developed in TUD and ULB was presented in [29,31–33], respectively. The starting time of the loading on AAS and AASF concrete was 8 h and 11 h, while for CEM I, CEM III/A and CEM III/B concrete, the starting time was 5.5 h, 5 h, and 7 h, respectively. The deformation threshold of AC and OC was 2 μm/m and 6.7 μm/m, respectively. When the deformation of the concrete exceeded that threshold, a load would be activated to pull or push the concrete back to the original position. The cycles succeeded to themselves during the entire test until the concrete cracked.

3. Results and discussion

3.1. Degree of reaction

The degrees of reaction of AC and OC mixtures with time are plotted in Fig. 2. It can be seen from Fig. 2 (a) that OC has a generally more complete reaction than AC in a month of curing. At the age of 3 days, the degrees of reaction of OC mixtures already exceed 0.8 while those of AC are still below 0.6. After 7 days, the reaction in OC is basically stabilized while the one in AC keeps increasing till 28 days. However, in the very early age, e.g., < 0.5d, the reaction degrees of AC systems are higher than those of OC systems as shown in Fig. 2 (b), which indicates a faster reaction rate of AC systems in this period. This information is consistent with the normally faster setting of AC than OC (see Tables 3 and 4) [34].

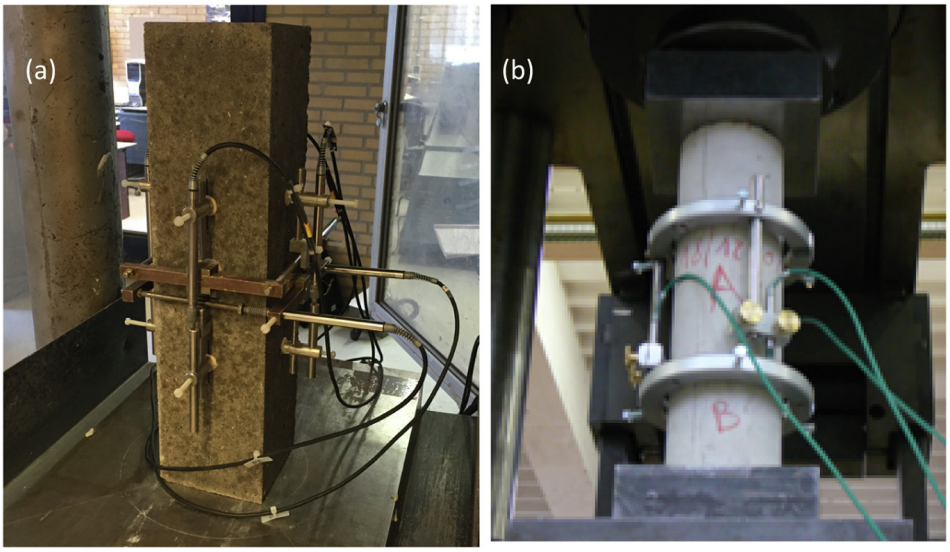

Fig. 1. Apparatus for elastic modulus measurements on AC (a) and OC (b).

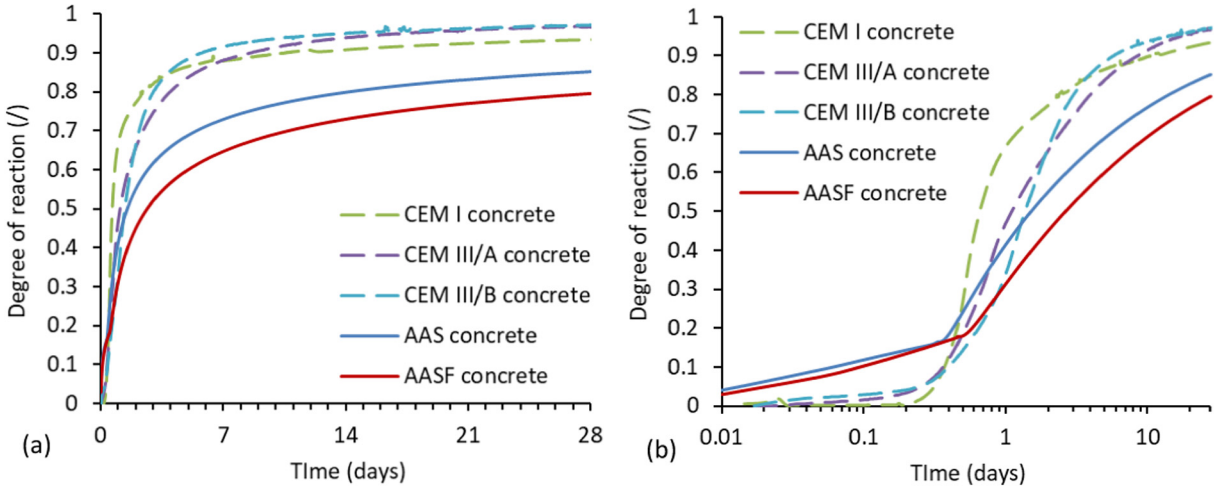

Fig. 2. Degree of reaction of AC (solid lines) and OC (dashed lines) with time in normal (a) or logarithmic scale (b).

3.2. Mechanical properties

3.2.1. Strength

3.2.1.1. Strength evolution with time. The comparison of the strength evolutions of AC and OC is shown in Fig. 3. AAS concrete has the fastest compressive strength development from 1 day to 7 days while AASF concrete has the slowest. After the 7th day, the increment in the compressive strength of OC turns slower than that of AC. The compressive strength of AASF concrete is always lower than that of AAS concrete due to the replacement of slag by fly ash. In contrast, using different clinkers has rather limited effect on the compressive strength of OC. At 28 days, AASF concrete shows similar strength to the ones of OC.

Despite the comparable compressive strength of AC and OC, the splitting strength of AC is lower than that of OC in the whole period studied. On 7 days, for example, the splitting tensile strength of OPC-based concrete mixtures is all above 5 MPa, while the one of AAS and AASF concrete reaches only 3.3 MPa and 2.4 MPa, respectively.

In Fig. 4, the splitting strength-to-compressive strength (f_t/f_c) ratios of AC and OC are plotted together. It can be seen that the f_t/f_c of CEM I concrete at all curing ages is around 0.1. For CEM III/A and CEM III/B concrete, the f_t/f_c fluctuates a bit in the first days but stabilizes at around 0.1 after 7 days. In contrast, AAS and AASF concretes show similar evolutions of f_t/f_c, which decrease from around 0.1 at the first day to only 0.06 till 28 days. These results reveal that AC is more prone to tensile failure than OC, which is in line with the findings from [34–36]. It seems that the commonly used f_t/f_c value, 0.1, to estimate the tensile strength of OC from its compressive strength is not applicable to AC.

The much lower f_t/f_c of AC compared to OC might be due to the development of microcracking within AC. As a porous and heterogenous material, the failure modes of concrete under tension and compression are different. While the compressive strength of concrete is mainly dependent on the (capillary) porosity of the solid skeleton, the splitting tensile strength is much more sensitive to microcracking. Due to the large autogenous shrinkage of AC (as will be shown in Fig. 9), there is a high potential of development of microcracks surrounding the rigid aggregates [37,38], which impairs the tensile strength more than the compressive strength. The development of microcracking could also reduce the stiffness of the concrete, as will be discussed in Section 3.2.2. Of course, the possibility is not excluded that the intrinsically tensile strength of C-A-S-H gel, the main reaction product in AAS and AASF, can be lower than that of C-S-H in OPC. However, few studies can be found comparing the sub-micro to molecular scale mechanical properties of the gels.

3.2.1.2. Strength evolution with degree of reaction. OPC and AAMs, as two intrinsically different systems, involve different chemical

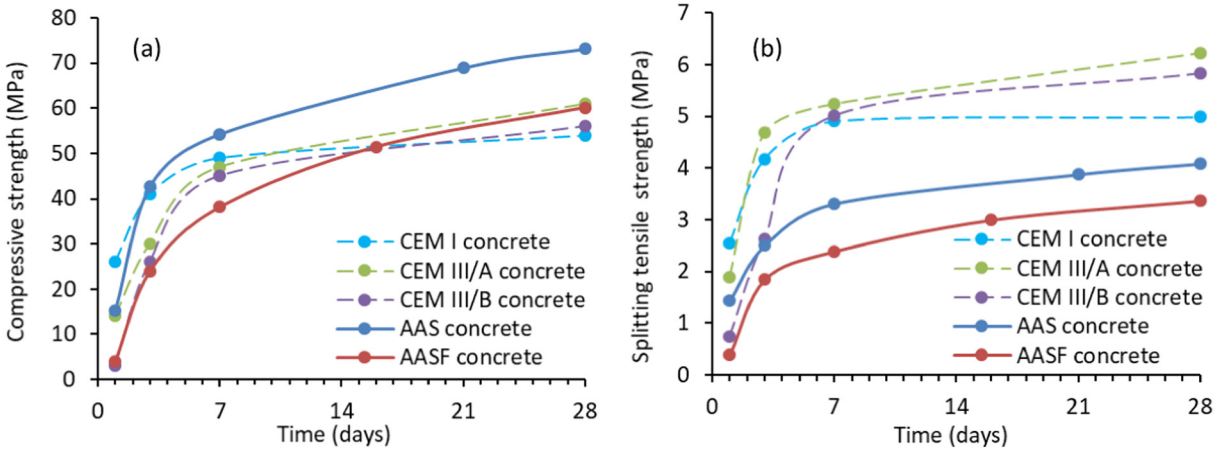

Fig. 3. Compressive strength (a) and splitting strength (b) of AC (solid lines) and OC (dashed lines).

processes and reaction kinetics. In fact, the mechanical properties of the concrete are dependent more on the degree of reaction than the curing age. In Fig. 5, the evolutions of the strength against degrees of reaction of the concrete are shown. It can be seen that there appear linear relationships between the strength and the degree of reaction of AC. This information can be very useful for establishing model codes to predict the compressive and splitting tensile strengths of AC. For OC mixtures, the strength trends with the increasing degrees of reaction are a bit scattered, indicating a larger influence of the binder compositions. Nonetheless, when the reaction degree is higher than 0.7, the slopes of the fitted lines for all mixtures are similar.

3.2.2. Elastic modulus

3.2.2.1. Elastic modulus evolution with time. The elastic modulus of AC and OC is shown in Fig. 6. Similar to the splitting tensile strength, the elastic modulus of AC is generally lower than that of OC. AASF concrete shows lower elastic modulus than AAS concrete. However, it is noted that the elastic modulus of AAS concrete starts to slightly decrease after 7 days. No decrease in elastic modulus is observed for OC mixtures. Like the decreased f_t/f_c of the concrete, the slight decrease in elastic modulus of AAS concrete is also believed to relate to the development of microcracking due to locally restrained autogenous shrinkage [37,39]. Elastic modulus is a parameter reflecting the stiffness of the material under load. With the increase of curing age, more reaction products are formed and denser structure is built within the concrete. Therefore, elastic modulus of concrete normally positively or even linearly relates to compressive strength for OC [40]. However, unlike compressive strength, elastic modulus involves also the deformational information of the material. When microcracking presents in the concrete, the compressive strength may be limited affected, but the strain of concrete under compressive or tensile stress would increase. In fact, the deformation due to the healing or slipping of microcracks in concrete may not be classified as "elastic" deformation [41], but when we use the term "elastic modulus" to reflect the overall stress-to-strain ratio of the concrete, a lower measured value would be obtained due to microcracking. Therefore, the elastic modulus value seems to be the result of the competition between the stiffening structure and the development of microcracking. In the age after 7 days, the degree of reaction of AAS concrete increases marginally (see Fig. 2) while its autogenous shrinkage keeps developing (as will be shown in Fig. 9), which results in a decreasing elastic modulus.

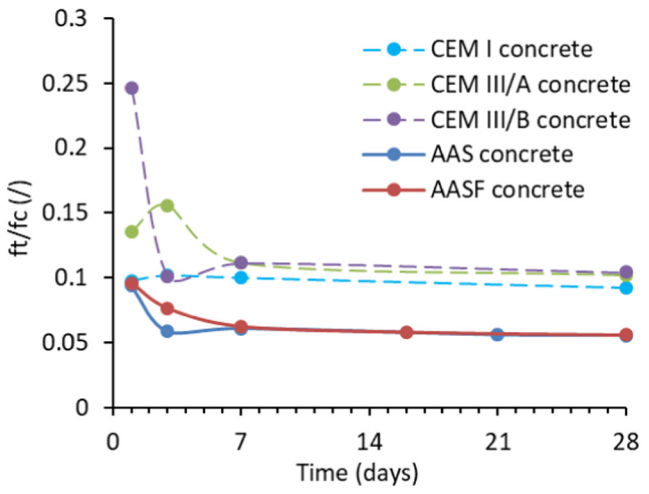

Fig. 4. Splitting strength-to-compressive strength (f_t/f_c) ratios of AC (solid lines) and OC (dashed lines).

3.2.2.2. Elastic modulus evolution with degree of reaction. When the elastic modulus of the concrete is plotted against degree of reaction, it can be seen that the curves for OC nearly overlap with each other, as shown in Fig. 7. By contrast, the elastic modulus of the two AC mixtures shows greatly different magnitudes at the same degree of reaction.

3.2.3. Modelling of the mechanical properties

For ordinary cement concrete compositions, several models have been developed to link the mechanical properties and the degree of reaction as explained in details in [42]. It was generally observed that a power law can be used to relate both parameters as expressed in Equation (1):

$$X(t) = X_\infty \left(\frac{\alpha(t) - \alpha_0}{1 - \alpha_0} \right)^a \quad (1)$$

where X is the studied mechanical properties, X_∞ is the ultimate value of the mechanical properties when the degree of reaction reaches 100%, α is the degree of reaction, α_0 is the degree of reaction at the zero time and a is a material parameter related to the kinetics of one mechanical property. For OC mixtures, the zero time is defined as the final setting time of the mixture (see Table 4) [30]. For AC, the starting time of the acceleration period is chosen as the zero time as suggested by [43]. For each property and composition, one amplitude and one kinetics parameters are used to define the development of the property according to degree of reaction.

The modelled mechanical properties of the concrete mixtures by Equation (1) are shown in Fig. 8. Even better correspondences are observed for AC mixtures than OC mixtures since very early age. This highlights the fact that such model can also be used for alkali activated materials.

Based on the results of the fitting (least square method), two main results are obtained: the final value of each properties X_∞ and the kinetics parameter a, as shown in Table 5. Generally speaking, the differences between the X_∞ values and the measured results for the age of 28 days are larger for AC mixtures than for OC mixtures. This indicates a higher potential of further improvements of mechanical properties of AC after 28 days. For the kinetics parameter a, it is observed on OC that the replacement of Portland clinker by slag generally increases the value of the kinetics parameter while a lower value is obtained for AAS concrete generally.

3.3. Autogenous shrinkage

The autogenous shrinkage of AC and OC is shown in Fig. 9. The autogenous shrinkage of AC is generally higher than that of OPC based concrete, except in the first day when CEM I concrete shows the rapidest development of autogenous shrinkage. AAS concrete shows higher autogenous shrinkage than AASF concrete. This is in line with the autogenous shrinkage results obtained on AAMs paste [43]. Another phenomenon observed from Fig. 9 is that CEM III/A and CEM III/B concrete mixtures experienced expansion at the very early age. This is due to the formation of crystalline reaction products such as portlandite and ettringite [44]. If the zero time of the curves for CEM III/A and CEM III/B is chosen as the end of the expanding age, the total autogenous shrinkage of the two mixtures would be larger, but still lower than that of AC. No expansion was observed in AC, since there was no expansive crystals formed in these materials [43].

3.4. Autogenous shrinkage-induced stress

Fig. 10 shows the stress developments in AC and OC measured by TSTMs. The cracking initiation of the concrete is indicated by the suddenly drop of the stress to around zero. The stress

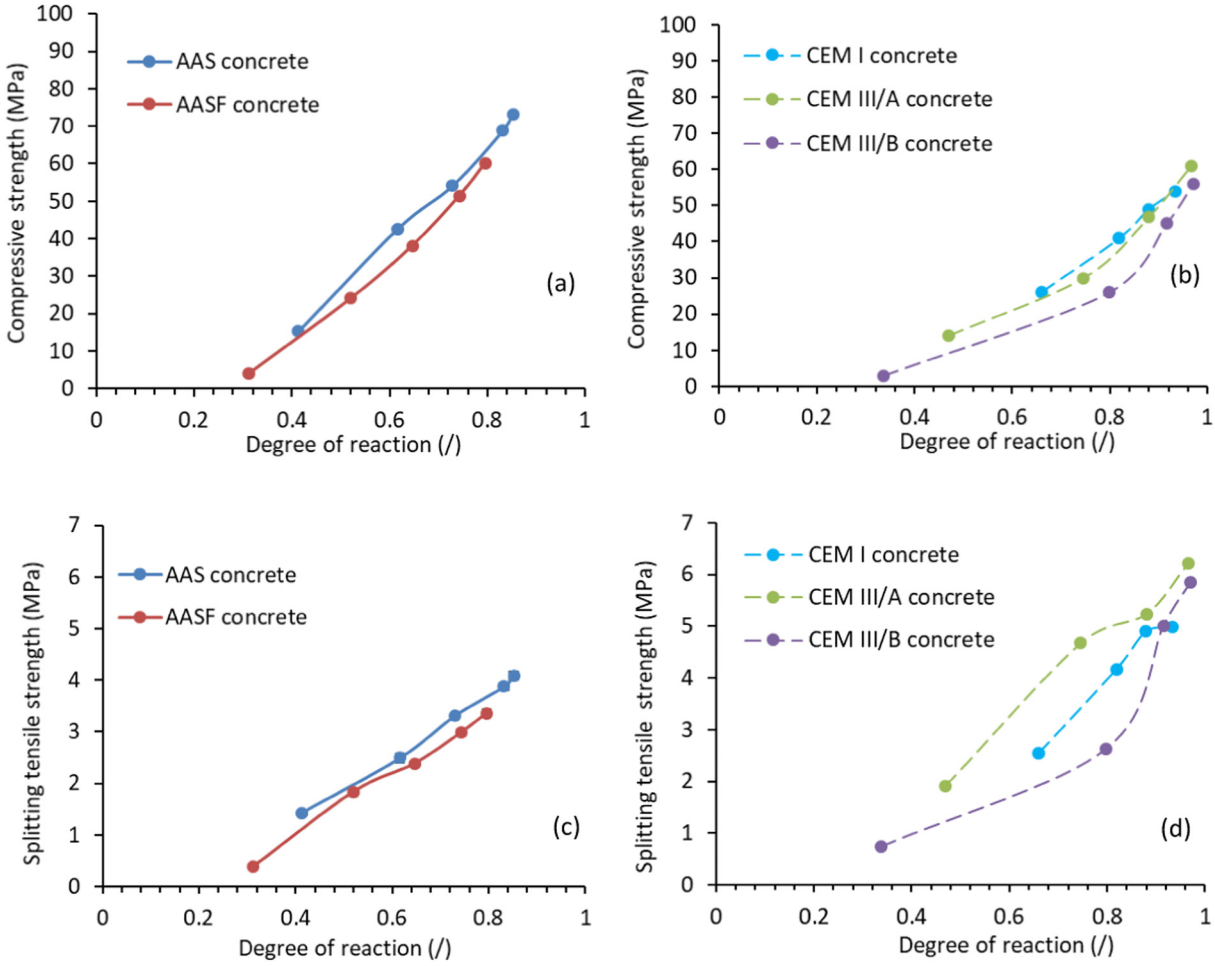

Fig. 5. Compressive strength and splitting strength evolutions of AC (a.c) and OC (b,d) with degree of reaction.

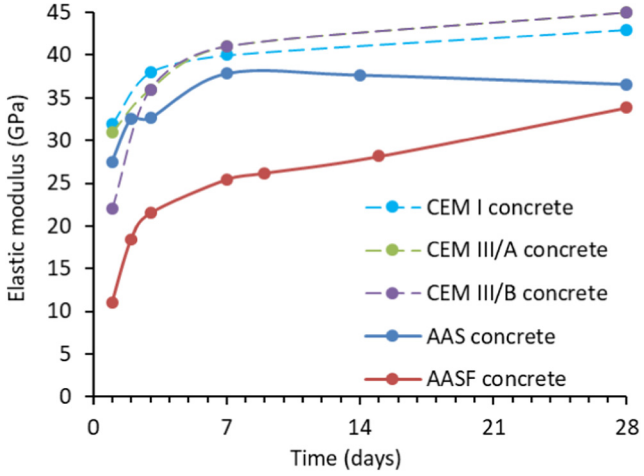

Fig. 6. Elastic modulus of AC (solid lines) and OC (dashed lines).

developing curves for OC are more stepwise than the curves for AC, which is because of the higher deformation threshold used in ULB than in TUD (see Section 2.2.5).

Among all mixtures, CEM I concrete experienced the fastest stress development, which is consistent with the high autogenous shrinkage of this mixture at the very early age. Cracking occurred in CEM I concrete when the stress reached 3 MPa. The tensile stress in CEM III/A and CEM III/B concrete did not develop at the first 1–2 days until the concrete started to show shrinkage. The tensile stresses at the failure of these two mixtures are similar to that of CEM I concrete.

The stress in AAS concrete also develops rapidly due to the high autogenous shrinkage, but the increasing rate of the stress turned lower than that for CEM I concrete after the first day, as shown in Fig. 10. The concrete did not crack until around 20 days. AASF concrete was not subject to considerable tensile stress until 1.5 days when the autogenous shrinkage started to rapidly develop. The lower autogenous shrinkage (see Fig. 9) and lower elastic modulus (see Fig. 6) of AASF concrete lead to a lower tensile stress than in AAS concrete, due. However, the tensile strength of AASF concrete was also lower than that of AAS concrete (see Fig. 3). In the end. Cracking occurred earlier in AASF concrete than AAS concrete.

Based on the cracking time and stress rate results, OC mixtures all show "high" cracking potential according to ASTM C1581 [45]. The cracking potential of AC mixtures, by contrast, belongs to "moderate-low" [45]. The lower cracking proneness of AC compared to OC within similar compressive strength is beneficial to widen the commercial acceptance of AC.

The reason why AC shows higher autogenous shrinkage but lower internal tensile stress than OC is probably attributed to the lower elastic modulus and the more evident creep and relaxation of AC. According to [46], slag based alkali-activated materials show pronounced viscoelasticity. This viscoelasticity contributes to the free autogenous shrinkage of AC and stress relaxation under restrained conditions.

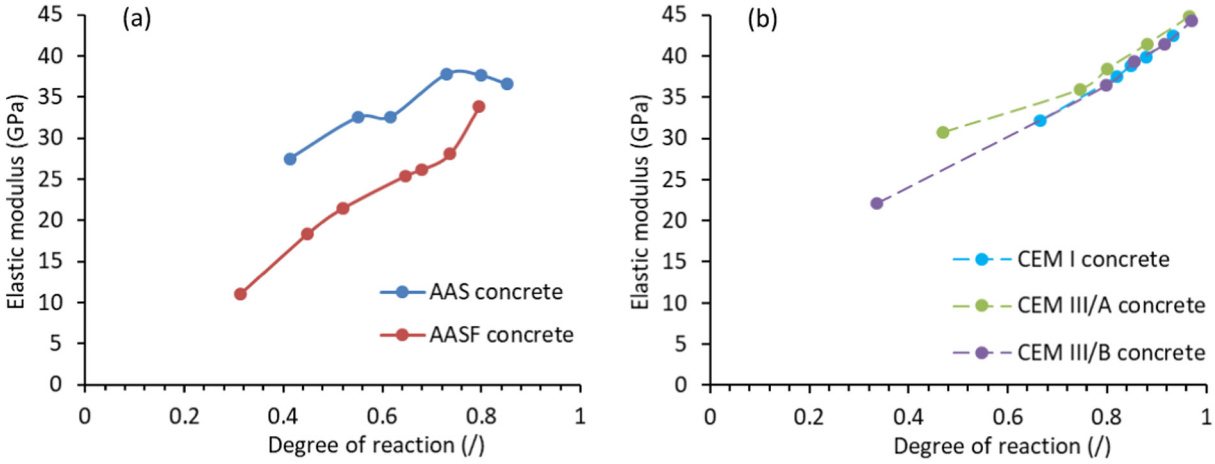

Fig. 7. Elastic modulus evolutions of AC (a) and OC (b) with degree of reaction.

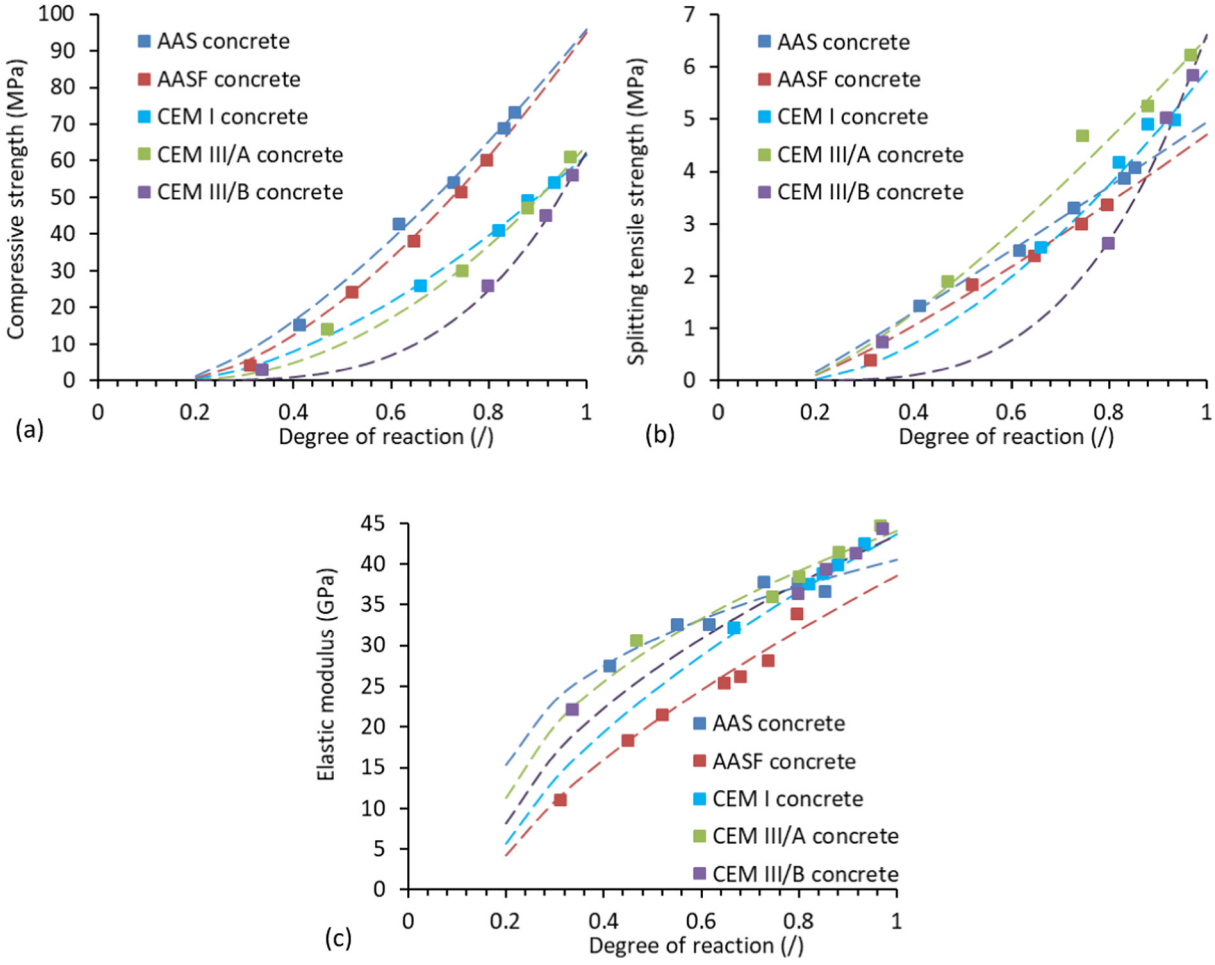

Fig. 8. Experimentally measured (dots) and modelled (dashed lines) compressive strength (a), splitting tensile strength (b) and elastic modulus (c) of all concrete mixtures.

It is also noted that the failing stresses of all concrete mixtures are lower than their splitting tensile strength at corresponding ages. This may be the result of size effect [47]. Since the beam is much longer than the cube, there is a high probability that some cross-sections in the beam have lower strength than the middle cross-section of the cube, whereas the strength of the beam is determined by the weakest cross-section.

From Fig. 11 where the stress evolutions are plotted against the degree of reaction, it can be seen that the cracking of CEM I, CEM III/A and AAS concrete occurred at rather similar degrees of reaction (around 0.83), although the cracking times of these concrete vary significantly. The degree of reaction of AASF at which the concrete breaks is 0.75, which is lowest one among all mixtures. The result in Fig. 11 reveals that part of the reason for the earlier

Table 5
Parameters of Equation (1) for the five concrete mixtures.

Mixtures	α_0	X_∞(MPa)			α(/)		
		f_c	f_t	E	f_c	f_t	E
AAS	0.17	95.8	4.95	40,484	1.40	1.05	0.31
AASF	0.18	94.9	4.71	38,620	1.61	1.18	0.69
CEM I	0.10	61.7	5.93	43,683	1.61	1.67	0.64
CEM III/A	0.10	64.1	6.55	44,089	2.03	1.27	0.43
CEM III/B	0.12	62.5	6.61	43,559	3.39	3.31	0.53

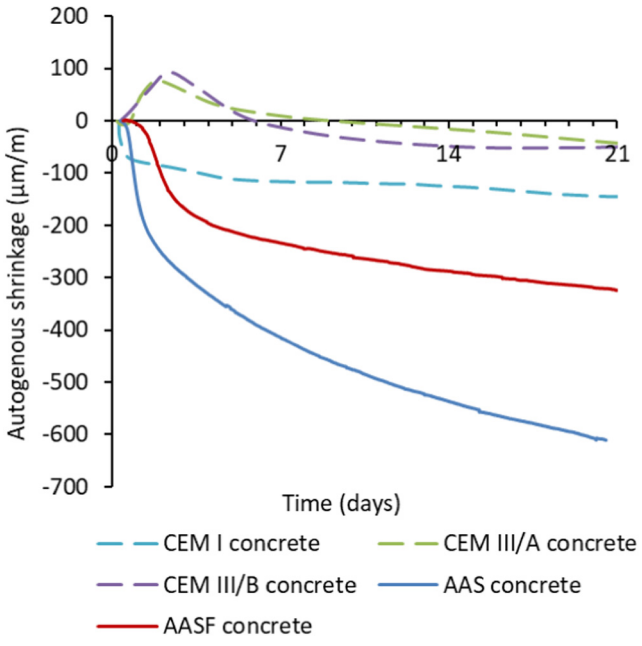

Fig. 9. Autogenous shrinkage of AC (solid lines) and OC (dashed lines).

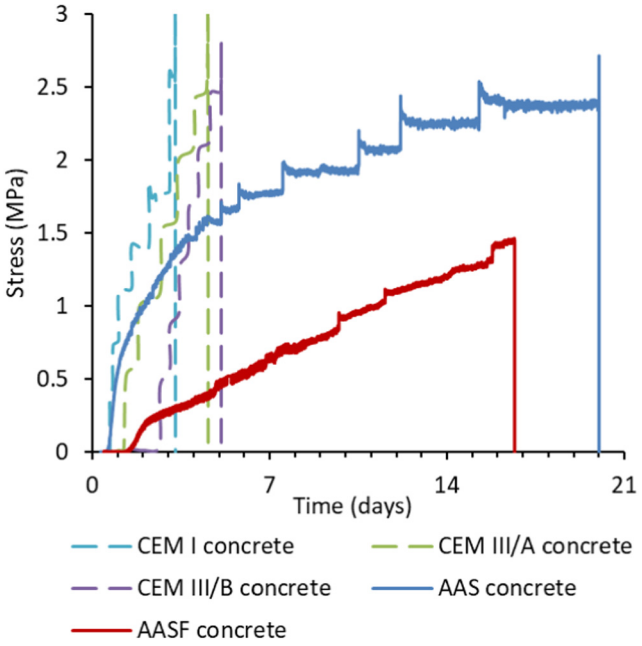

Fig. 10. Autogenous shrinkage-induced stress in AC (solid lines) and OC (dashed lines).

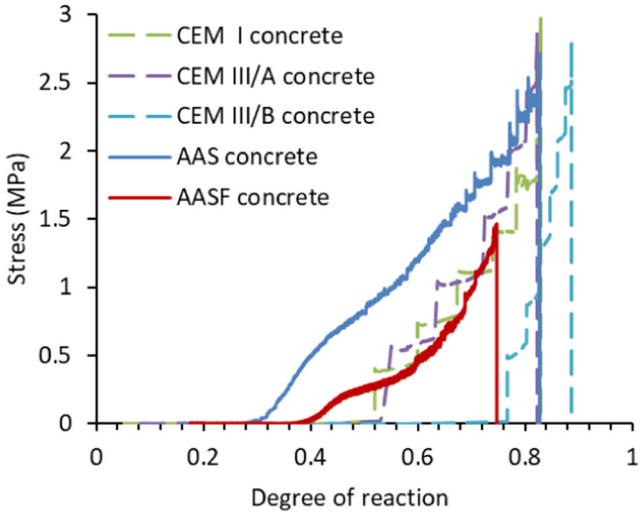

Fig. 11. Autogenous shrinkage-induced stress in AC (solid lines) and OC (dashed lines) with degree of reaction.

cracking in OC than AC may lie in the faster reactions in OC in the early age. Indicated by this, reducing the reaction rate in the early age may be a strategy to mitigate the cracking potential of the concrete.

3.5. Creep coefficient

As discussed in the last section, the low stress in AC is partially contributed by relaxation resulting from the viscoelasticity of the material. The concrete viscoelasticity can be reflected by the creep coefficient, i.e., the ratio between creep and elastic deformation, of the concrete [48]. The parallel experiments conducted on free autogenous shrinkage and restrained autogenous shrinkage enable the separation of creep strain from the total deformation.

If drying and thermal effects are not involved, the strain of a concrete under load is contributed by three components: autogenous shrinkage, elastic deformation, and creep. For concrete under fully restrained conditions, the total deformation is supposed to be zero, as shown by Equation (2). The strain evolution of the concrete in TSTM is schematically shown in Fig. 12. The autogenous shrinkage, when exceeds the strain threshold, is compensated by the elastic deformation and the creep driven by the load provided by the TSTM.

$$\varepsilon(t) = \varepsilon_{el}(t) + \varepsilon_{cr}(t) - \varepsilon_{as}(t) = 0 \tag{2}$$

where$\varepsilon(t)$ is the strain of the concrete. $\varepsilon_{as}(t)$ is the autogenous shrinkage of the concrete (see Fig. 9). $\varepsilon_{el}(t)$ and $\varepsilon_{cr}(t)$ are the elastic deformation and creep of the concrete under tensile stress provided by the TSTM.

The elastic strain of the concrete can be calculated by Equation (3).

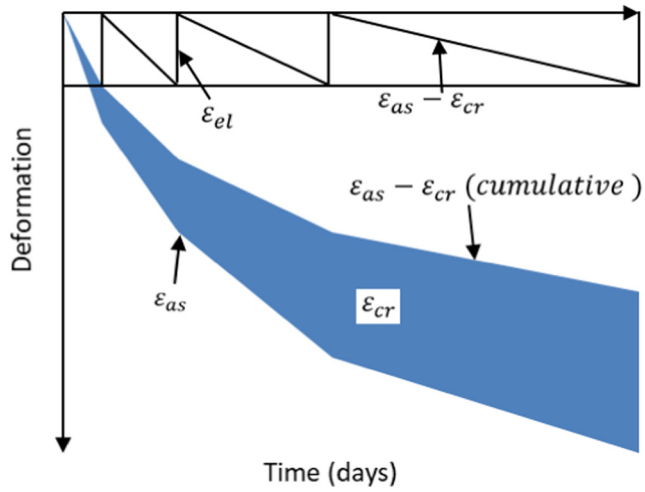

Fig. 12. Schematic representation of the shrinkage-compensation cycles to obtain a fully restrained condition by TSTM.

$$\varepsilon_{el}(t) = \frac{\sigma(t)}{E(t)} \quad (3)$$

where $\sigma(t)$ is the stress (see Fig. 10) and $E(t)$ is the elastic modulus of the concrete (see Fig. 6).

The correspondingly calculated elastic and creep strains of all concrete mixtures are shown in Supporting Information.

The creep coefficient $\varnothing$(t) of the concrete can be calculated by Equation (4).

$$\varnothing(\mathrm{t}) = \frac{\varepsilon_{cr}(t)}{\varepsilon_{el}(t)} \quad (4)$$

It should be noted that the definition of the creep coefficient as shown in Equation (4) is different from the common definition, which is usually the ratio between the creep strain at a fixed age and the instantaneous strain at the start of loading. In the present study, the elastic deformation is not a constant value, but corresponds to the strain at the time considered [48].

According to Equations 2–4, the creep coefficients of AC and OC under tensile stress are calculated and shown in Fig. 13. The creep coefficient of the concrete during expansion is not considered.

It can be seen that CEM III/A concrete and CEM/IIIB concrete show very low creep coefficient, which means the deformation under the tensile stress provided by TSTM to compensate the autogenous shrinkage is basically elastic. The creep coefficient of CEM I concrete is around 2 at the first day and decreases to around 1 afterwards. This is consistent with the results of [15,49,50], where creep coefficients of 1–2 were reported for CEM I based systems.

In contrast, AC mixtures show creep coefficients higher than 6 after the second day. The large creep coefficients of AAS and AASF concrete obtained in this study are in accordance with the evident creep/relaxation of AAMs systems reported in [51–53]. According to [51], the stacking regularity of C-A-S-H layers is reduced due to the structural incorporation of alkali cations into C-A-S-H gel, which is easier to collapse and redistribute compared with C-S-H gel in OPC. As a result, AAS and AASF systems show evident viscoelastic behaviours. When the concrete restrained, the viscoelasticity contributes to the relaxation of the stress and a later cracking of the concrete.

4. Conclusions

In this study, the mechanical properties, autogenous shrinkage and cracking proneness of AC and OC are compared. The main findings are summarised as following:

(1) AC mixtures show higher reaction rates than OC mixtures in the first hours, which contribute to the fast setting of AC. Afterwards, the degree of reaction of OC is higher than AC until 28 days. This results in a fast development of compressive strength of OC. The splitting strength-to-compressive strength ratio of AC is lower than that of OC, which indicates that AC is more prone to tensile failure.
(2) AAS concrete shows similar elastic modulus to OC during the first week of reaction. Afterwards, the elastic modulus of AAS concrete decreases, which is not observed in other mixtures. The elastic modulus of AASF concrete is the lowest among all the mixtures in the whole period studied.

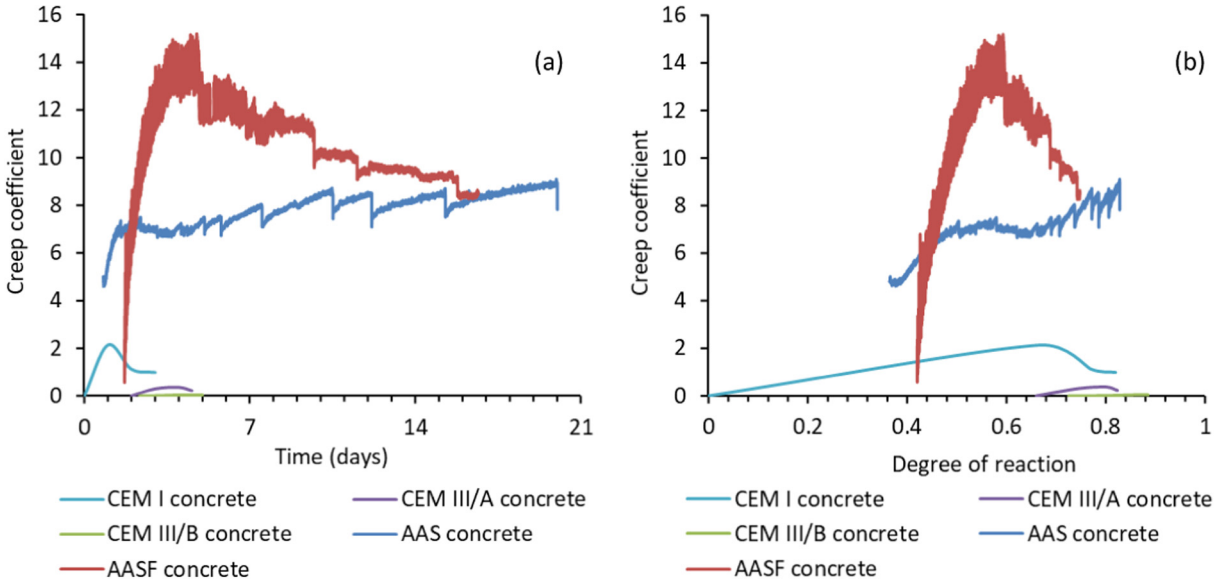

Fig. 13. Creep coefficient of AC and OC with time (a) or with degree of reaction (b) during the period of loading by TSTM. The creep coefficient in the stage when the concrete shows expansion is not taken into consideration.

(3) The mechanical properties of AC correspond to a power law when expressed in function of the reaction degree like OC. The amplitude and kinetics parameters used for this model are generally lower for AC in comparison to OC, except for the compressive strength.
(4) AC shows higher autogenous shrinkage than OC. While the autogenous shrinkage of OC becomes stable after 7 days, the one of AC keeps increasing at high rates till three weeks.
(5) Despite the higher autogenous shrinkage of AC, the stress generated in restrained AC is lower than in OC. The cracking of AC occurred much later than that of OC. Nonetheless, the degrees of reaction at which AAS concrete and OC cracked are very similar. This indicates that reducing the reaction rate of AC might be a strategy to mitigate the cracking proneness of the concrete.
(6) The low stress in restrained AC is partially due to the relaxation resulting from the evident viscoelasticity of the material. This point is verified by the much higher creep coefficient of AC in comparison to OC.

CRediT authorship contribution statement

Zhenming Li: Conceptualization, Methodology, Investigation, Writing - original draft, Writing - review & editing. **Brice Delsaute:** Conceptualization, Investigation, Writing - review & editing. **Tianshi Lu:** Methodology. **Albina Kostiuchenko:** Investigation. **Stéphanie Staquet:** Supervision. **Guang Ye:** Supervision, Writing - review & editing, Writing - review & editing.

Declaration of Competing Interest

The authors declare that they have no known competing financial interests or personal relationships that could have appeared to influence the work reported in this paper.

Acknowledgment

Zhenming Li was supported by the China Scholarship Council (CSC) under grant No. 201506120072 and Netherlands Organisation for Scientific Research (NWO) under grant No. 15803. Brice Delsaute would like to acknowledge the Belgian National Fund for Scientific Research (FRS-FNRS) in the frame of the Interact project. Klaas van Breugel is acknowledged for his valuable suggestions and discussion on creep and relaxation.

Appendix A. Supplementary data

Supplementary data to this article can be found online at https://doi.org/10.1016/j.conbuildmat.2021.123418.

References

[1] J.I. Escalante-Garcia, L.J. Espinoza-Perez, A. Gorokhovsky, L.Y. Gomez-Zamorano, Coarse blast furnace slag as a cementitious material, comparative study as a partial replacement of Portland cement and as an alkali activated cement, Constr. Build. Mater. 23 (2009) 2511–2517.
[2] E. Worrell, L. Price, N. Martin, C. Hendriks, L.O. Meida, Carbon dioxide emissions from the global cement industry, Annu. Rev. Energy Environ. 26 (2001) 303–329.
[3] K.L. Scrivener, R.J. Kirkpatrick, Innovation in use and research on cementitious material, Cem. Concr. Res. 38 (2008) 128–136, https://doi.org/10.1016/J.CEMCONRES.2007.09.025.
[4] C. Shi, A.F. Jiménez, A. Palomo, New cements for the 21st century: The pursuit of an alternative to Portland cement, Cem. Concr. Res. 41 (2011) 750–763, https://doi.org/10.1016/j.cemconres.2011.03.016.
[5] P. Duxson, J.S.J. Van Deventer, Commercialization of geopolymers for construction – opportunities and obstacles, Geopolymers. (2009) 379–400, https://doi.org/10.1533/9781845696382.3.379.
[6] J.L. Provis, J.S.J. Van Deventer, Geopolymers: structures, processing, properties and industrial applications, Woodhead, Cambridge, UK, 2009.
[7] K. Arbi, M. Nedeljković, Y. Zuo, G. Ye, A Review on the Durability of Alkali-Activated Fly Ash/Slag Systems: Advances, Issues, and Perspectives, Ind. Eng. Chem. Res. 55 (2016) 5439–5453, https://doi.org/10.1021/acs.iecr.6b00559.
[8] M.C.G. Juenger, F. Winnefeld, J.L. Provis, J.H. Ideker, Advances in alternative cementitious binders, Cem. Concr. Res. 41 (2011) 1232–1243, https://doi.org/10.1016/j.cemconres.2010.11.012.
[9] C. Cartwright, F. Rajabipour, A. Radli, Shrinkage Characteristics of Alkali-Activated Slag Cements, J. Mater. Civ. Eng. 27 (2014) 1–9, https://doi.org/10.1061/(ASCE)MT.1943-5533.0001058.
[10] M. Hojati, Shrinkage characteristics of alkali activated fly ash-slag binders, The Pennsylvania State University, 2014.
[11] M. Hojati, A. Radlińska, Shrinkage and strength development of alkali-activated fly ash-slag binary cements, Constr. Build. Mater. 150 (2017) 808–816, https://doi.org/10.1016/j.conbuildmat.2017.06.040.
[12] N.K. Lee, J.G. Jang, H.K. Lee, Shrinkage characteristics of alkali-activated fly ash/slag paste and mortar at early ages, Cem. Concr. Compos. 53 (2014) 239–248, https://doi.org/10.1016/j.cemconcomp.2014.07.007.
[13] S. Uppalapati, S. Joseph, Ö. Cizer, AUTOGENOUS SHRINKAGE AND STRENGTH DEVELOPMENT OF ALKALI-ACTIVATED SLAG/FLY ASH MORTAR BLENDS, in: 5th Int. Slag Valoris. Symp., 2017: pp. 393–396.
[14] Z. Li, M. Nedeljkovic, Y. Zuo, G. Ye, Autogenous shrinkage of alkali-activated slag-fly ash pastes, in: 5th Int. Slag Valoris. Symp., Leuven, 2017: pp. 369–372.
[15] P. Lura, Autogenous Deformation and Internal Curing of Concrete, Delft University of Technology, 2003.
[16] F. Collins, J.G. Sanjayan, cracking tendency of alkali-activated slag concrete subjected to restrained shrinkage, Cem. Concr. Res. 30 (2000) 791–798, https://doi.org/10.1016/S0008-8846(00)00243-X.
[17] ASTM C618 - 19, Standard specification for coal fly ash and raw or calcined natural pozzolan for use in concrete, (2008). doi:10.1520/C0618-19.2.
[18] A. Darquennes, Comportement au jeune âge de bétons formulés à base de ciment au laitier de haut-fourneau en condition de déformations libre et restreinte, Université libre de Bruxelles, Thèse de doctorat, 2009.
[19] Z. Li, S. Zhang, X. Liang, G. Ye, Cracking potential of alkali-activated slag and fly ash concrete subjected to restrained autogenous shrinkage, Cem. Concr. Compos. 114 (2020), https://doi.org/10.1016/j.cemconcomp.2020.103767 103767.
[20] A. Darquennes, B. Espion, S. Staquet, How to assess the hydration of slag cement concretes?, Constr Build. Mater. 40 (2013) 1012–1020, https://doi.org/10.1016/j.conbuildmat.2012.09.087.
[21] NEN-EN 12390-3, Testing hardened concrete - Part 3: Compressive strength of test specimens, (2009).
[22] NBN B 15-220, Essais des bétons - Détermination de la résistance à la compression., (1990).
[23] NBN B 15-218, Essais des bétons - Détermination de la résistance à la traction par fendage, (1986).
[24] NEN-EN 206-1, Concrete - Part 1: Specification, performance, production and conformity, Eur. Comm. Stand. (2001).
[25] N. Zabihi, Effect of specimen size and shape on strength of concrete, Eastern Mediterranean University (EMU) (2012).
[26] NBN B 15-203, Essais des bétons - Module d'élasticité statique en compression, (1990).
[27] C. Boulay, S. Staquet, B. Delsaute, J. Carette, M. Crespini, O. Yazoghli-Marzouk, É. Merliot, S. Ramanich, How to monitor the modulus of elasticity of concrete, automatically since the earliest age?, Mater. Struct. 47 (2014) 141–155.
[28] B. Delsaute, C. Boulay, J. Granja, J. Carette, M. Azenha, C. Dumoulin, G. Karaiskos, A. Deraemaeker, S. Staquet, Testing Concrete E-modulus at Very Early Ages Through Several Techniques: An Inter-laboratory Comparison, Strain. (2016) 91–109, https://doi.org/10.1111/str.12172.
[29] S.J. Lokhorst, Deformational behaviour of concrete influenced by hydration related changes of the microstructure, Delft University of Technology, 2001.
[30] A. Darquennes, S. Staquet, M.P. Delplancke-Ogletree, B. Espion, Effect of autogenous deformation on the cracking risk of slag cement concretes, Cem. Concr. Compos. 33 (2011) 368–379, https://doi.org/10.1016/j.cemconcomp.2010.12.003.
[31] Z. Li, X. Yao, Y. Chen, T. Lu, G. Ye, A low-autogenous-shrinkage alkali-activated slag and fly ash concrete, Appl. Sci. 10 (2020) 6092, https://doi.org/10.3390/app10176092.
[32] S. Staquet, B. Delsaute, A. Darquennes, B. Espion, Design of a Revisited Tstm System for Testing Concrete Since Setting Time Under Free and Restraint Conditions, CONCRACK 3 – RILEM-JCI Int. Work. Crack Control Mass Concr. Relat. Issues Concern. Early-Age Concr. Struct. 15-16 March 2012, Paris, Fr. (2012) 12.
[33] B. Delsaute, S. Staquet, Testing Concrete Since Setting Time Under Free and Restrained Conditions, in: Adv. Tech. Test. Cem. Mater., Springer, 2020: pp. 177–209.
[34] M. Nedeljković, Z. Li, G. Ye, Setting, Strength, and Autogenous Shrinkage of Alkali-Activated Fly Ash and Slag Pastes: Effect of Slag Content, Materials (Basel). 11 (2018) 2121, https://doi.org/10.3390/ma11112121.
[35] M.H. Hubler, J.J. Thomas, H.M. Jennings, Influence of nucleation seeding on the hydration kinetics and compressive strength of alkali activated slag paste, Cem. Concr. Res. 41 (2011) 842–846.
[36] F. Collins, J.G. Sanjayan, Microcracking and strength development of alkali activated slag concrete, Cem. Concr. Compos. 23 (2001) 345–352, https://doi.org/10.1016/S0958-9465(01)00003-8.

[37] Z. Li, T. Lu, Y. Chen, B. Wu, G. Ye, Prediction of the autogenous shrinkage and microcracking of alkali-activated slag and fly ash concrete, Cem. Concr. Compos. 117 (2021), https://doi.org/10.1016/j.cemconcomp.2020.103913.
[38] Z. Li, M. Nedeljković, B. Chen, G. Ye, Mitigating the autogenous shrinkage of alkali-activated slag by metakaolin, Cem. Concr. Res. 122 (2019) 30–41, https://doi.org/10.1016/j.cemconres.2019.04.016.
[39] S. Prinsse, D.A. Hordijk, G. Ye, P. Lagendijk, M. Luković, Time-dependent material properties and reinforced beams behavior of two alkali-activated types of concrete, Struct. Concr. 21 (2020) 642–658, https://doi.org/10.1002/suco.201900235.
[40] A.M. Neville, Properties of Concrete, Longman, London, 2011.
[41] W. Lyu, Effect of micro-cracking and self-healing on long-term creep and strength development of concrete, Delft University of Technology, 2020.
[42] F. Benboudjema, J. Carette, B. Delsaute, T.H. de Faria, A. Knoppik, L. Lacarrière, A.N. de Mendonça Lopes, P. Rossi, S. Staquet, Mechanical properties, in: Therm. Crack. Massive Concr. Struct., Springer, 2019, pp. 69–114.
[43] Z. Li, T. Lu, X. Liang, H. Dong, J. Granja, M. Azenha, G. Ye, Mechanisms of autogenous shrinkage of alkali-activated slag and fly ash pastes, Cem. Concr. Res. 135 (2020), https://doi.org/10.1016/j.cemconres.2020.106107 106107.
[44] S. Zhutovsky, K. Kovler, A. Bentur, Influence of cement paste matrix properties on the autogenous curing of high-performance concrete, Cem. Concr. Compos. 26 (2004) 499–507.
[45] ASTM C 1581, Standard Test Method for Determining Age at Cracking and Induced Tensile Stress Characteristics of Mortar and Concrete under Restrained Shrinkage, ASTM Int. (2009) 1–7. doi:10.1520/C1581.
[46] T.C. Hansen, Creep and stress relaxation of concrete: a theoretical and experimental investigation, Svenska forskningsinstitutet för cement och betong vid Kungl, Tekniska högskolan, 1960.
[47] Z.P. Bazant, J. Planas, Fracture and size effect in concrete and other quasibrittle materials, CRC Press, 1997.
[48] K. Kovler, Testing system for determining the mechanical behaviour of early age concrete under restrained and free uniaxial shrinkage, Mater. Struct. 27 (1994) 324–330, https://doi.org/10.1007/BF02473424.
[49] Z. Hu, Early hydration and shrinkage of alkali-activated slag/fly ash blend cement, Hunan University (2013).
[50] T. Lu, Autogenous shrinkage of early age cement paste and mortar, Delft University of Technology, 2019.
[51] H. Ye, A. Radlińska, Shrinkage mechanisms of alkali-activated slag, Cem. Concr. Res. 88 (2016) 126–135, https://doi.org/10.1016/j.cemconres.2016.07.001.
[52] Z. Li, J. Liu, G. Ye, Drying shrinkage of alkali-activated slag and fly ash concrete; A comparative study with ordinary Portland cement concrete, Heron. 64 (2019) 149.
[53] A. Kostiuchenko, Z. Li, G. Ye, Experimental study on creep behavior of alkali-activated concrete, in: Int. Conf. Innov. Mater. Sustain. Civ. Eng., Nanjing, 2019: p. 80.